A Fast Calculation Method of Iron Losses of PWM inverter-Fed Motor in Heat Generation Control for Powertrain of Parked BEV

Takahiro Kumagai [1)] Masahiro Takemoto [1)] Kenji Inokuma [1)]
Yoshiyuki Kimura [1)] Keisuke Kawai [1)]

1) DENSO Corporation, Aichi, Japan
E-mail: takahiro.kumagai.j2x@jp.denso.com

ABSTRACT: This paper proposes a fast calculation method for the motor iron loss which is one of the heat sources in the specific control in order to generate a heat source for heater and battery heating by conducting a current into the powertrain of the parked battery electric vehicle (BEV), which is so-called "heat generation control" in this paper. This first process is to create two databases (A) for low-frequency iron loss calculated with a current source simulating a current control system and (B) for high-frequency iron loss calculated with a voltage source simulating a PWM inverter, with a finite element analysis (FEA). Next, the motor iron loss is calculated by referring to those two databases depending on the control parameters and condition in the heat generation control, which realizes the fast calculation. In comparison with a general iron loss calculation by combining a control/circuit simulation and a FEA, the calculation time is reduced by 93% while maintaining an accuracy of 5.4% error rate at 1p.u. current amplitude.

KEY WORDS: battery electric vehicle, thermal management, powertrain, motor, iron loss, pulse wide modulation

1. INTRODUCTION

Environmental regulations towards carbon neutrality accelerate the spread of BEVs in society worldwide. However, short cruising distance and long charging time of BEVs are major problems in widespread adoption(1).

Fig.1 explains the battery temperature characteristic causing the problems of BEVs(1). In low-temperature environment, the battery input/output power is limited due to the temperature characteristic of lithium-ion batteries. In addition, BEVs, which cannot use wasted heat in engine, increase the electricity consumption due to use of heater of air conditioner. As a result, the deterioration of cruising distance and charging time becomes obvious. Therefore, thermal management is necessary to generate a heat source and utilize its heat source optimally for heater and batter heating.

Fig.2 explains the thermal system with heat generation control in the powertrain of the parked BEV(1). The installation of electric high voltage heater in order to generate a heat source leads to increased vehicle cost and compressed interior space(2). Therefore, as shown in Fig.2, heat sources in the already installed powertrain such as inverters and motors are utilized for heater and battery heating through the water circuit. Especially in parked BEV, since the power train is not driven and does not generate a heat source, specific control in order to intentionally generate a heat source is necessary, which is so-call "heat generation control".

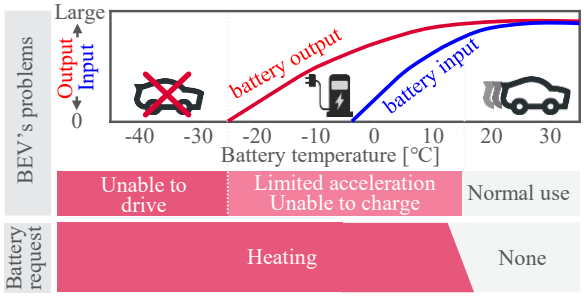

Fig.1 Battery temperature characteristic causing the problems of BEVs(1)

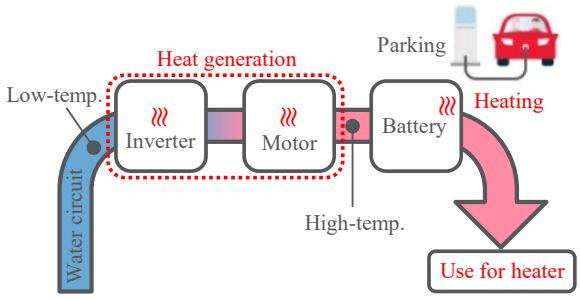

Fig.2 Thermal system with heat generation control in the powertrain of the parked BEV

In general heat generation control of the powertrain in the parked BEV, the d-axis current or zero-phase current, which does not contribute to torque, is conducted in order to generate only losses with no torque(3)(4). In particular, specific control to conduct

an alternating current (AC) into d-axis does not require an additional system and generate a large amount of heat source, which is so-called “d-axis AC heat generation control” in this paper. In this control, the amount of generated heat source depends on the several conditions and control parameters. In order to maximize the amount of generated heat source, these control parameters have to be adjusted to simultaneously heat all parts of the powertrain up to their respective temperature limits during both the parking with the heat generation control and the driving immediately after the end of this control. In particular, it is assumed that the parameters are intentionally adjusted to increase only harmonic losses associated with pulse width modulation (PWM). Therefore, the calculation of losses (i.e., amount of generated heat source) considering PWM is essential.

In general, the losses considering PWM is calculated by combining a control/circuit simulator and a FEA[5][6]. However, long computation time per one case is required due to the large number of analysis steps in order to consider the PWM effects. In addition, many cases have to be calculated in order to adjust the multiple parameters to maximize the amount of generated heat source. As a result, the computation time of multiple parameters optimizations becomes long.

In order to reduce the computation time to calculate the loss considering PWM, several calculation methods have been proposed. For the inverter losses, the calculation methods with some mathematical equation and no-simulator have already been proposed[7][8]. In those methods, the inverter losses are calculated from the switching device’s characteristic and several condition such as current amplitude, power supply voltage, switching frequency, and modulation index. On the other hand, for the motor losses, the copper loss is easily calculated from the current root-mean-square (RMS) value, while the iron loss cannot be easily calculated due to their complexity. There are some approaches to calculate the iron loss with mathematical equation such as Steinmetz equation and its improvements[9]-[16]. However, it is necessary to obtain the time variation data of the magnetic flux density at each part of the iron core in order to calculate the absolute amount of iron loss of the motor. In the other words, it is difficult to calculate the absolute amount of iron loss only by mathematical equation without FEA.

Therefore, a fast calculation method for iron loss considering PWM is proposed without the computation time per one case in d-axis AC heat generation control. This proposed method achieves fast calculation while estimating absolute amount of iron loss with FEA. This first process is to create two databases (A) for low-frequency iron loss calculated with a current source simulating a current control system and (B) for high-frequency iron loss calculated with a voltage source simulating a PWM inverter, with a FEA, and the reason for this process is explained in Chapter 2.2 and 3.2. Next, the iron loss is calculated by referring to those two databases depending on the control parameters and condition, which realizes the fast calculation.

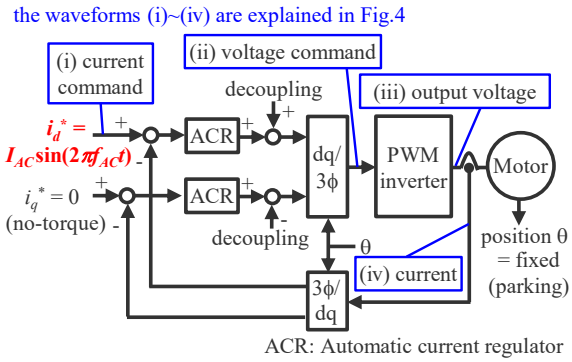

Fig.3. Control block of the d-axis AC heat generation control

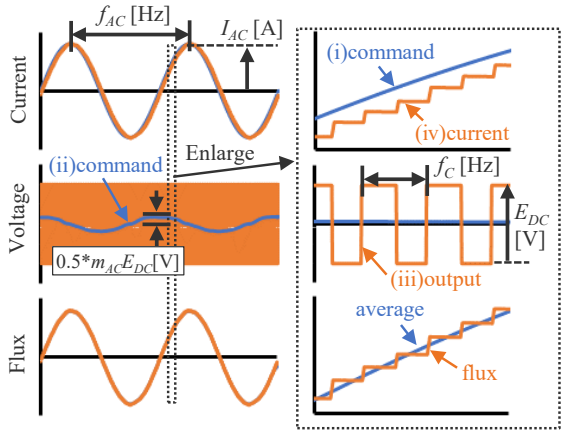

Fig.4 Some waveforms in the d-axis AC heat generation control

2. HEAT GENERATION CONTROL in PARKED BEV

As mentioned in Chapter 1, a heat generation control is essential in parked BEV. In particular, d-axis AC heat generation control is focused. In Chapter2, first, the detail of d-axis AC heat generation control is explained, next, the factor to determine the amount of generated heat source and calculation method are explained.

2.1. Heat generation control for power train

Fig.3 shows the control block of the d-axis AC heat generation control. As shown in Fig.3, only d-axis AC current which does not contribute to torque is conducted in order to generate only losses with no output in parked BEV. This control does not require an additional system and generates a large amount of heat source compared with other methods[3][4]. In order to maximize the amount of generated heat sources, it is necessary to simultaneously

heat all parts of the powertrain up to their respective temperature limits during both the parking with the heat generation control and the driving immediately after the end of this control. Therefore, it is essential to organize the factors to determine the amount of generated heat source in this control and to calculate it.

2.2. Factors determining amount of generated heat source

Fig.4 shows some waveforms in the d-axis AC heat generation control. As shown in Fig.3, the d-axis current is controlled to AC with the frequency f_{AC} [Hz] and the amplitude I_{AC} [A] with automatic current regulation (ACR) and PWM inverter. As a result, the copper loss of $3/2*R*I_{AC}^2$ occurs in the motor with three-phase winding resistance R. In addition, the magnetic flux varies with time at f_{AC}. As a result, low-frequency iron loss occurs in the motor. Note that the distribution of current to UVW changes depending on the electric angle θ[deg] at park, which also affects these losses. In addition, the inverter drives with PWM. As a result, harmonic components in the carrier frequency f_c [Hz] are generated in the current and magnetic flux. Generally, this harmonic component changes depending on not only f_c but also the power supply voltage E_{dc} [V] and the modulation index of AC voltage m_{AC}. High-frequency copper loss and iron loss occur depending on the magnitude of this harmonic component. In general, under to the condition of f_c of 10^3-10^4 Hz, f_{AC} is 10^1-10^2 Hz due to the ACR frequency band or the concerns of the noise and vibration due to electromagnetic excitation force.

2.3. Calculation of amount of generated heat source

To summarize Section 2.2, the amount of generated heat source is determined by the copper and iron losses due to fundamental and harmonic components, which are changed by six conditions or parameters: f_{AC}, I_{AC}, θ, f_c, E_{dc}, and m_{AC}. In order to maximize the amount of generated heat source, it is necessary to calculate it associated with these parameters. While a formula-base method for inverter losses has been established[7], only a few studies have been reported on for motor loss, especially iron loss. In generally, the iron loss is calculated by combining a control/circuit simulator and FEA.

3. IRON LOSS CALCULATION Considering PWM

3.1. General iron loss calculation[5][6]

Fig.5 shows a flowchart of a general iron loss calculation method. In general FEA, the iron loss is analyzed with a current source since the analysis with voltage source coupling a control/circuit simulator directly is too time consuming.

First, as shown in #1 of Fig.5, a motor plant model for the control/circuit simulator is created from a 2D/3D motor model.

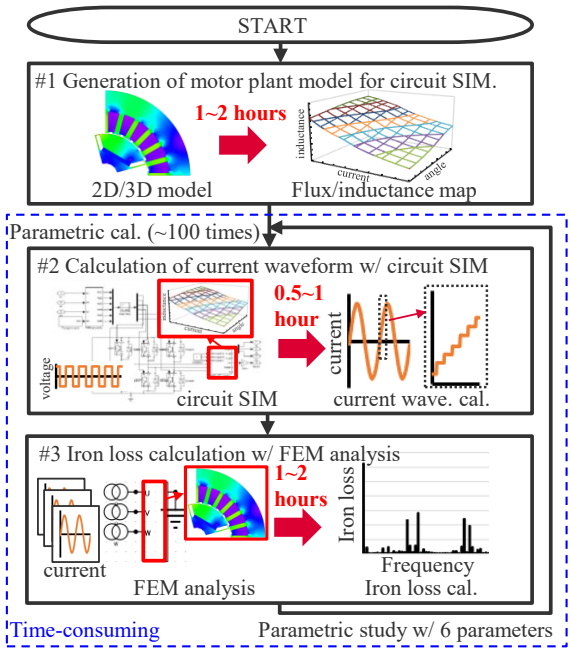

Fig.5 Flowchart of general iron loss calculation method[5][6]

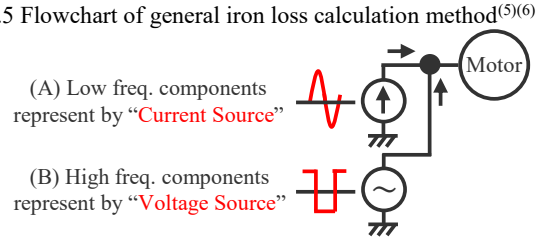

Fig.6 Concept of the proposed method

Next, as shown in #2 of Fig.5, current waveform considering PWM is derived with the control/circuit simulator with both the created motor plant model and a total of six conditions and parameters (f_{AC}, I_{AC}, θ, f_c, E_{dc}, and m_{AC}).

Finally, as shown in #3 of Fig.5, the current waveform is input to a 2D/3D motor model using a current source, and the iron loss is calculated by FEA. Note that the simulation time has to be longer than $1/f_{AC}$, while the step width has to be sufficiently shorter than $1/f_c$. As a result, the number of analysis steps becomes large, and the computation time of multiple parameters optimizations becomes long.

3.2. Proposed iron loss calculation

Fig.6 explains the concept of the proposed iron loss calculation method. The key to the proposed method is to clearly separate the inputs into (A) low frequency and (B) high frequency and consider them separately. In particular, as discussed in section 2.2, (A) the input of low-frequency component of f_{AC} is regarded as the current which controlling the command current by ACR. In other words, it is regarded as the current source realizing the current command. On the other hand, (B) the input of the frequency component of f_c is generated by PWM voltage output by an inverter. In other words, it is regarded as the voltage source realizing the voltage subtracting

the command component (i.e., low frequency component) from the PWM inverter output.

Fig.7 shows a flowchart of a proposed iron loss calculation method.

First, as shown in #1 in Fig.7, the iron loss is calculated with FEA by inputting the current source realizing the current command. Since the low-frequency iron loss is considered to depend on f_{AC}, I_{AC}, and θ as described in section 2.2, the iron loss is associated with these three parameters in DB.

Next, as shown in #2 in Fig.7, the high frequency iron loss is calculated by FEA by inputting the voltage source subtracting the command component (i.e., low frequency component) from the PWM inverter output. Since the high-frequency iron loss is considered to depend on f_c, E_{dc}, and m_{AC} as described in section 2.2, the iron loss is associated with these three parameters in DB. Note that the analysis is for one pulse in the PWM inverter output at the modulation index of DC voltage m_{DC}. This analysis is with the simulation time of f_c and the small number of analysis steps. This is because the analysis at the modulation index of AC voltage m_{AC} with the simulation time of f_{AC} is the large number of analysis steps. As an alternative, it is necessary for this method to convert the iron loss of m_{DC} into the iron loss of m_{AC}. At first, the analyzed iron loss of m_{DC} is approximated by third-order polynomial in Eq.(1).

$$W_i(m_{DC}) = a_{DC3}m_{DC}^3 + a_{DC2}m_{DC}^2 + a_{DC1}m_{DC}^1 \quad \cdots\cdots (1)$$

Note that a_{DC1}, a_{DC2}, and a_{DC3} are first, second, and third order coefficient in the polynomial equation respectively. Next, assuming that the modulation waveform of AC voltage is m_{AC} *sinθ_{AC}, the iron loss of m_{AC} is equal to the value obtained by substituting m_{AC} *sinθ_{AC} into Eq.(1) and taking the periodic average, and expressed as in Eq.(2).

$$\overline{W_i(m_{AC})} = \frac{1}{\pi}\int_0^{\pi} W_i(m_{AC}sin\theta_{AC})d\theta_{AC}$$
$$= \frac{1}{\pi}\left(\frac{4}{3}a_{DC3}m_{AC}^3 + \frac{\pi}{2}a_{DC2}m_{AC}^2 + 2a_{DC1}m_{AC}^1\right) \quad (2)$$

As shown in Eq.(2), the iron loss is calculated from the modulation index of AC voltage m_{AC} and the a_{DC1}, a_{DC2}, and a_{DC3} which are obtained with the analysis is for one pulse in the PWM inverter output at the modulation index of DC voltage m_{DC}. On the other words, this process need not require the long number of analyses as general iron loss calculation.

Finally, as shown in #3 in Fig.7, depending on the six conditions and parameters, the total iron loss is calculated by referring to the low-frequency and high-frequency iron loss based on the above two DBs and adding them together. Note that m_{AC} is automatically

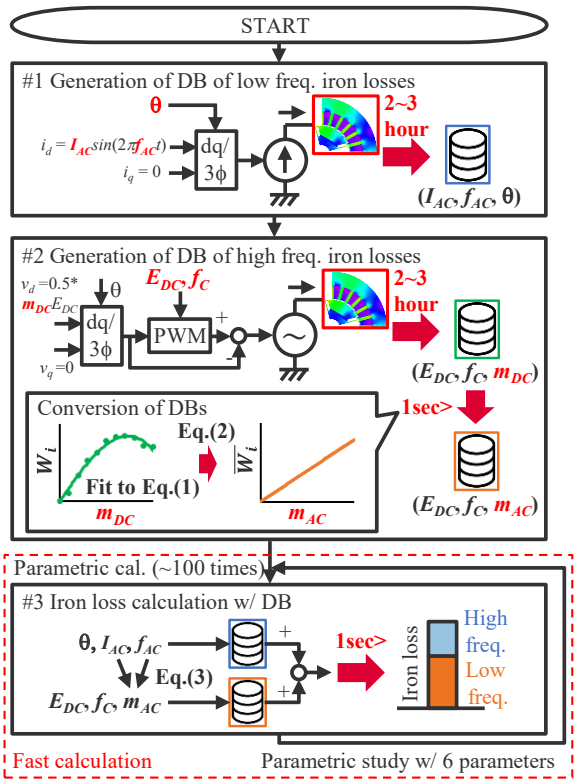

Fig.7 Flowchart of proposed iron loss calculation method

determined with Eq.(3) base on several condition (The derivation is shown in the appendix).

$$m_{AC} = \frac{V_{AC}}{E_{dc}/2} = \frac{\sqrt{2/3}\sqrt{(RI_{AC})^2+(2\pi f_{AC}L_dI_{AC})^2}}{E_{dc}/2} \quad \cdots\cdots (3)$$

In this method, DB creation also has only one frequency component, so it is constructed relatively quickly. In addition, after the DB construction, the parametric calculation for maximizing the amount of generated heat sources is done quickly even if there are many trials. This is because the one trial is only referring the two DBs and adding together according to the six conditions and parameters.

4. VERIFICATION RESULTS

This section explains the accuracy of the proposed method and the effects on reducing the computation time. MATLAB/Simulink is used for control/circuit simulation in the general method, and JMAG-Designer is used for FEA. For the iron loss analysis, the FFT method is used.

4.1. Accuracy

Fig. 8 shows the results of the accuracy verification. Note that there are two condition of the switching frequency (a)5kHz and (b)20kHz. In addition, the AC current amplitude is varied for comparative verification. In comparison with a general iron loss calculation by combining a control/circuit simulation and a FEA,

the error rates of the proposed method under the condition of a current amplitude of 1 p.u. are 3.5% and 5.4% for two condition of the switching frequency (a)5kHz and (b)20kHz respectively, indicating high accuracy.

4.2. Computation time

Fig. 9 shows a comparison of computation times. In this case, the comparison is made for a parametric calculation to maximize the amount of generated heat source for six conditions and parameters. It is also assumed that 60 cases of calculations are required using the design of experiment method. As shown in Fig.9, the simulation time is very time consuming for the general method. On the other hand, the proposed method takes a relatively long time to create the DB, but even with 60 cases, the calculation is completed in a short time because the iron loss is calculated at high speed. As a result, the calculation time is reduced by about 93%.

5. CONCLUSIONS

This paper proposes a fast calculation method for the motor iron loss which is one of the heat sources in the specific control in order to generate a heat source for heater and battery heating by conducting a current into the powertrain of the parked BEV. This first process is to create two databases (A) for low-frequency iron loss calculated with a current source simulating a current control system and (B) for high-frequency iron loss calculated with a voltage source simulating a PWM inverter, with a FEA. Next, the motor iron loss is calculated by referring to those two databases depending on the control parameters and condition in the heat generation control, which realized the fast calculation. Comparing with a general iron loss calculation by combining a control/circuit simulation and a FEA, the calculation time is reduced by 93% while maintaining an accuracy of 5.4% error rate at 1p.u. current amplitude.

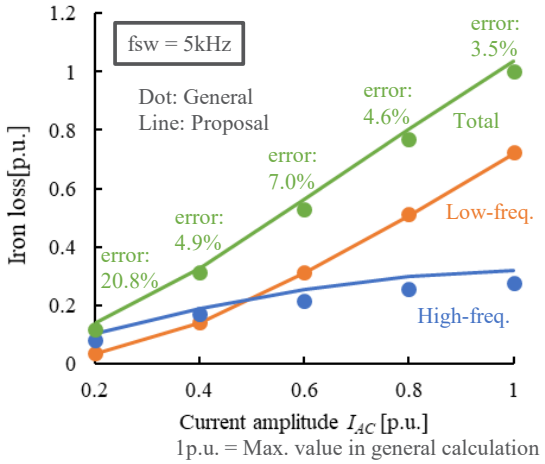

(a) Switching frequency: 5kHz

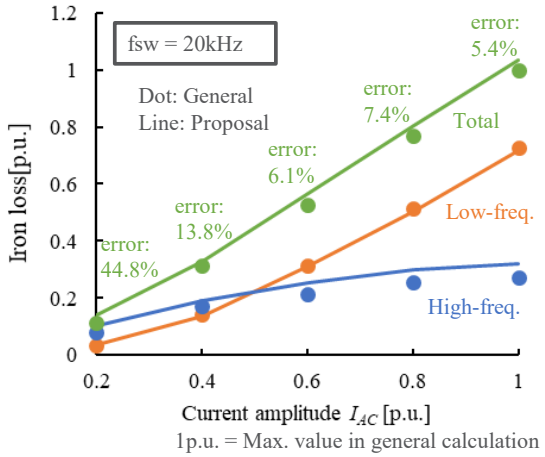

(b) Switching frequency: 20kHz

Fig.8 Comparison result of calculated iron loss

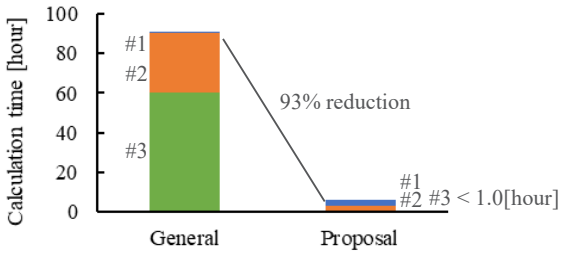

Fig.9 Comparison result of calculation time

REFERENCES

(1) M. Numata: “Trend of Thermal Management Technology for Electric Vehicles”, DENSO TECHNICAL REVIEW, Vol.28, (2023) (in Japanese)

(2) X. Hu, et al: “Battery warm-up methodologies at subzero temperatures for automotive applications: Recent advances and perspectives”, Prog. Energy and Combustion Science, Vol.77, No.100806, pp.1–28 (2020)

(3) R. Hasegawa, K. Kondo, C. Funayama, and A. Imura: “Internal Battery Heating Method in Electric Vehicles During Storrage via D-axis Current Palsation”, PE-24-040, PSE-24-052, SPC-24-094 (2024) (in Japanese)

(4) BYD Company Limited, JP 2022-540373 (2022,9,15)

(5) Y. Shimizu, S. Motimoto, M. Sanada, and Y. Inoue: “Influence of Carrier Harmonics on Performance of IPMSMs for Automotive Applicaions”, Journal of the Japan Institute of Power Electronics, Vol.43, pp.130–137 (2017)

(6) JSOL Corporation. “Products>JMAG-RT.” https://www.jmag-international.com/products/jmag-rt/ (accessed Oct 31, 2024).

(7) W. Deng, Y. Zhao, and J. Wu: “Energy Efficiency Improvement via Bus Voltage Control of Inverter for

Electric Vehicles", IEEE Transactions on Vehicular Technology, Vol.66, No.2, pp.1063–1073 (2017)

(8) Y. Kashihara and J. Itoh: "Performance Comparison of the Efficiency and Power Density among Multilevel Converter Topologies for a PV Inverter by the Pareto-Front Curve", IEEJ Transactions on Industry Applications, Vol.134, No.2, pp.209–219 (2014)

(9) C.I. McClay and S. Williamson: "The variation of cage motor losses with skew", IEEE Transactions on Industry Applications, vol. 36, no. 6, pp. 1563-1570 (2000)

(10) N. Sadowski, M. Lajoie-Mazenc, J.P.A. Bastos, M.V. Ferreira da Luz, and P. Kuo-Peng: "Evaluation and analysis of iron losses in electrical machines using the rain-flow method", IEEE Transactions on Magnetics, vol. 36, no. 4, pp. 1923-1926 (2000)

(11) Z. Gmyrek, A. Boglietti, an A. Cavagnino: "Estimation of Iron Losses in Induction Motors: Calculation Method, Results, and Analysis", IEEE Transactions on Industrial Electronics, vol. 57, no. 1, pp. 161-171 (2009)

(12) M. Nakahara and K. Wada: "Loss Analysis of Magnetic Components for a Solid-State-Transformer", IEEJ Journal Industry Applications, vol. 4, no. 4, pp. 387-397 (2015)

(13) L. Chang, W. Lee, T. M. Jahns, and K. Rahman: "Investigation and Prediction of High-Frequency Iron Loss in Lamination Steels Driven by Voltage-Source Inverters Using Wide-Bandgap Switches", IEEE Transactions on Industry Applications, vol. 57, no. 4, pp. 3607-3618 (2021)

(14) A. Boglietti, A. Cavagnino, D. M. Ionel, M. Popescu, D. A. Staton, and S. Vaschetto: "A General Model to Predict the Iron Losses in PWM Inverter-Fed Induction Motors", IEEE Transactions on Industry Applications, vol. 46, no. 5, pp. 1882-1890 (2010)

(15) M. Popescu, D. M. Ionel, A. Boglietti, A. Cavagnino, C. Cossar, and M. I. McGilp: "A General Model for Estimating the Laminated Steel Losses Under PWM Voltage Supply", IEEE Transactions on Industry Applications, vol. 46, no. 4, pp. 1389-1396 (2010)

(16) T. Kumagai, T. Itoh, K. Nishikawa, J. Itoh, K. Yamane, M. Nawa: "Reduction of Iron Loss in Stator Core using an Optimum Pulse Pattern for High-Speed IPMSM", IEEJ Transactions on Industry Applications, Vol. 141, No. 4, pp. 313-323 (2021)

APPENDIX

1. Derivation of Eq.(3)

The voltage equation of interior permanent magnet synchronous motor (IPMSM) in the parked BEV, i.e., zero motor rotational speed, is expressed as (A-1).

$$\begin{bmatrix} v_d \\ v_q \end{bmatrix} = R \begin{bmatrix} i_d \\ i_q \end{bmatrix} + \begin{bmatrix} L_d & 0 \\ 0 & L_q \end{bmatrix} \frac{d}{dt} \begin{bmatrix} i_d \\ i_q \end{bmatrix} \quad \text{(A-1)}$$

In the d-axis AC heat generation control as shown in Fig.3, the current is expressed as (A-2).

$$\begin{bmatrix} i_d \\ i_q \end{bmatrix} = \begin{bmatrix} I_{AC} \sin(2\pi f_{AC} t) \\ 0 \end{bmatrix} \quad \text{(A-2)}$$

By substituting equation (A-2) into Eq.(A-1) in order to derive the voltage amplitude, it becomes Eq. (A-3).

$$V_{AC} = \sqrt{\frac{2}{3}} \sqrt{v_d^2 + v_q^2} = \sqrt{\frac{2}{3}} \sqrt{(R I_{AC})^2 + (2\pi f_{AC} L_d I_{AC})^2} \quad \text{(A-3)}$$